

Journal of Organometallic Chemistry, 127 (1977) 245–260
 © Elsevier Sequoia S.A., Lausanne — Printed in The Netherlands

**CRYSTAL AND MOLECULAR STRUCTURE OF
 (η^3 -ALLYL)CARBONYLCHLOROBIS(DIMETHYLPHENYLPHOSPHINE)-
 IRIDIUM(III) HEXAFLUOROPHOSPHATE,
 $[\text{Ir}(\eta^3\text{-C}_3\text{H}_5)\text{Cl}(\text{CO})(\text{P}(\text{CH}_3)_2(\text{C}_6\text{H}_5))_2][\text{PF}_6]$**

JAMES A. KADUK, ARTHUR T. POULOS and JAMES A. IBERS *

Department of Chemistry, Northwestern University, Evanston, Illinois, 60201

(Received July 13th, 1976)

Summary

The structure of (η^3 -allyl)carbonylchlorobis(dimethylphenylphosphine)-iridium(III) hexafluorophosphate, $[\text{Ir}(\eta^3\text{-C}_3\text{H}_5)\text{Cl}(\text{CO})(\text{P}(\text{CH}_3)_2(\text{C}_6\text{H}_5))_2][\text{PF}_6]$, has been determined from three-dimensional X-ray data to add support for a proposed mechanism of the oxidative addition of allyl halides to $\text{IrX}(\text{CO})(\text{PR}_3)_2$ ($X = \text{halide}$). The compound crystallizes in space group $C_{2h}^5\text{-P}2_1/c$ with four formula units in a cell of dimensions $a = 11.027(1)$, $b = 12.230(2)$, $c = 19.447(5)$ Å, and $\beta = 103.16(2)^\circ$. Least-squares refinement of the structure has led to a value of the conventional R index (on F) of 0.066 for the 3018 independent reflections having $F_o^2 > 3\sigma(F_o^2)$. The crystal structure consists of discrete, monomeric ions. The hexafluorophosphate anion is disordered. The coordination geometry around the iridium atom may be described as octahedral, with the chloro ligand *trans* to the carbonyl group and each phosphorus atom *trans* to a terminal carbon of the allyl group. Structural parameters: Ir–P = 2.366(4), 2.347(3); Ir–Cl = 2.389(3); Ir–C(allyl) = 2.28(1), 2.24(1), 2.25(1); Ir–C(carbonyl) = 1.85(1) Å; P–Ir–P = 105.7(1); C(terminal)–Ir–C(terminal) = 66.2(8); C–C–C = 125(2)°. The allyl group makes an angle of 126° with the P–Ir–P plane. Correlations between geometric structure and number of d electrons are noted among several $\text{M-C}_3\text{H}_5^-$ complexes, and are interpreted in the light of theoretical models of the $\text{M-C}_3\text{H}_5^-$ bond.

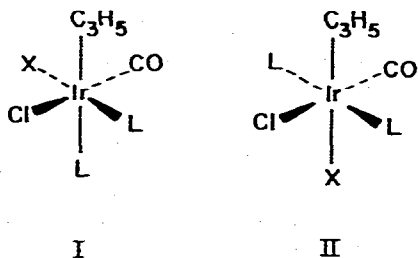
Introduction

A number of mechanisms have been proposed for the oxidative addition of alkyl halides to low-valent transition metal complexes, including nucleophilic attack of the metal at the carbon atom bearing the halogen [1,2], concerted insertion of the metal into the carbon–halogen bond [3], a radical chain process

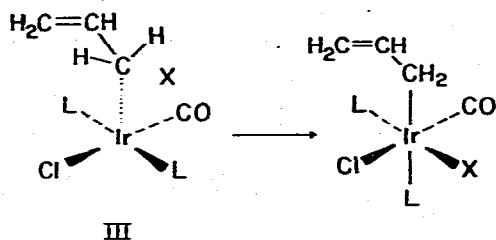
[4,5], and initial coordination of the double bond to the metal in the addition of alkenyl halides [6].

Many mechanistic studies have been made on $\text{IrX}(\text{CO})(\text{PR}_3)_2$ ($\text{X} = \text{halide}$) complexes [7], although none has established the stereochemistry of addition of the reactive carbon atom. The report by Osborn [6] that known radical scavengers inhibit the reaction with some alkyl halides (but not CH_3I , $\text{C}_6\text{H}_5\text{CH}_2\text{Cl}$, and $\text{CH}_2=\text{CHCH}_2\text{X}$) suggests that a free-radical pathway is not universal.

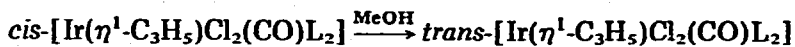
The observation of Deeming and Shaw [8] that allylic halides add to $\text{IrCl}(\text{CO})(\text{PMe}_2\text{Ph})_2$ and $\text{IrCl}(\text{CO})(\text{AsMe}_2\text{Ph})_2$ ($\text{Ph} = \text{C}_6\text{H}_5$) in benzene to form six-coordinate octahedral complexes with the allyl and halide ligands *cis* to each other (I) rather than *trans* (II) suggests that the reaction may proceed by con-



certed insertion of the iridium(I) complex into the carbon-halogen bond (III), leading to *cis*-addition as expected from orbital symmetry arguments [3]. How-



ever, kinetic and product studies using alkyl-substituted allyl halides suggest olefinic coordination to the iridium atom in the rate-determining step (IV) [9] (Fig. 1). This could lead to the formation of a π -allyliridium(III) intermediate or transition state (V) followed by attack of the displaced halide to yield the *cis*-adduct (Fig. 1). Complexes of the form V have been proposed as intermediates in the isomerization reaction of I to II [8].



$\text{L} = \text{PMe}_2\text{Ph}$ or AsMe_2Ph

The structures of such complexes in solution have been studied through proton magnetic resonance spectroscopy. Identification of an intermediate of the form V in the oxidative addition of allyl halides to complexes of the type $\text{IrX}(\text{CO})(\text{PR}_3)_2$ in benzene and proof of its structure would be strong evidence for the proposed mechanism [9]. Such a proof is presented here and the $\text{Ir}(\eta^3\text{-C}_3\text{H}_5^-)$ structure is compared with other known metal- π -allyl structures [10-26].

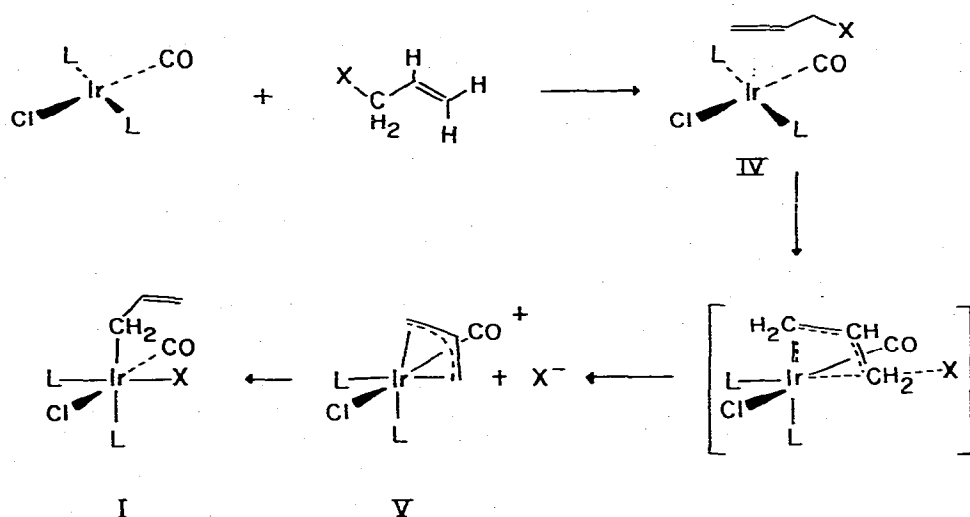


Fig. 1. Proposed mechanism for the addition of allyl halides to $\text{IrCl}(\text{CO})\text{L}_2$.

Experimental

Addition of hexafluorophosphate ion to a methanolic solution of II results in a precipitate of the presumed π -allyl complex (V) [8]. When this complex is dissolved in benzene and reacted with bromide ion, the *cis*-adduct (I) is obtained — a product identical with that of the oxidative addition of allyl bromide to $\text{IrCl}(\text{CO})(\text{PMe}_2\text{Ph})_2$ in benzene. Since the products and solvents are identical in the two reactions, the evidence is very good that V is an intermediate in the oxidative addition reaction.

A suitable crystal of V with approximate dimensions $0.45 \times 0.20 \times 0.20$ mm was selected from those produced in the reaction, and mounted at the end of a glass fiber. On the basis of optical goniometry and X-ray measurements, the principal faces were identified as belonging to the forms $\{100\}$, $\{010\}$, $\{001\}$, $\{10\bar{1}\}$, $\{101\}$, $\{011\}$ and $\{10\bar{2}\}$. On the basis of Weissenberg photography using Ni-filtered $\text{Cu-K}\alpha$ radiation, it was established that the crystal belongs to the monoclinic system. The observed extinctions $l = 2n + 1$ for $h0l$ and $k = 2n + 1$ for $0k0$ are consistent with the space group $C_{2h}^2-P2_1/c$. The lattice constants at 22° , which were determined from a least-squares refinement of the setting angles of 13 strong reflections which had been centered manually on a Picker FACS-I diffractometer using $\text{Cu-K}\alpha_1$ radiation ($\lambda = 1.540562 \text{ \AA}$), are $a = 11.027(1)$, $b = 12.230(2)$, $c = 19.477(5) \text{ \AA}$, and $\beta = 103.16(2)^\circ$. The density calculated for four formula weights per unit cell is 1.94 g cm^{-3} , which may be compared with the value of $1.86(3) \text{ g cm}^{-3}$ measured by suspending the crystals in a mixture of 1,3-dibromopropane and hexane.

For data collection using $\text{Cu-K}\alpha$ radiation was used. The intensities were measured by the $\theta-2\theta$ technique at a takeoff angle of 3° . At this angle the intensity of a reflection was about 90% of its maximum value as a function of takeoff angle.

A receiving counter aperture 6 mm high and 6 mm wide was used and was positioned 35 cm from the crystal. Asymmetric scans in 2θ , 1.8° below the K_{α_1} peak to 0.8° above the K_{α_2} peak, were used because of pronounced tailing of the diffraction peaks. Stationary-counter, stationary-crystal background counts of 10 sec for $2\theta < 80^\circ$ and 20 sec for $2\theta \geq 80^\circ$ were measured at the beginning and end of each scan. Attenuators were inserted automatically if the intensity of the diffracted beam exceeded about 7000 counts sec^{-1} .

The unique data set having $2\theta < 125^\circ$ was gathered; the intensities of 4423 reflections were recorded. The intensities of four standard reflections, measured after every 100 reflections, remained constant within counting statistics.

All data processing was carried out as previously described [27]. The value of p was selected as 0.04. The values of I and $\sigma(I)$ were corrected for Lorentz and polarization effects. Of the 4423 reflections, 3018 are unique, have $F_o^2 > 3\sigma(F_o^2)$, and were used in subsequent calculations. The linear absorption coefficient, μ , for this compound using Cu-K_α radiation is 137.9 cm^{-1} . An absorption correction was made and transmission coefficients ranged from 0.052 to 0.198.

The position of the iridium atom was unambiguously revealed by a Patterson synthesis. A least-squares refinement on F was computed* and the function $\sum w(|F_o| - |F_c|)^2$ was minimized, in which $w = 4F_o^2/\sigma^2(F_o^2)$ and $|F_o|$ and $|F_c|$ are the observed and calculated structure amplitudes. Values of the atomic scattering factors and anomalous terms were taken from the usual source [29]. Only the positional parameters of the iridium atom and the overall scale factor were varied, and the refinement gave the agreement indices $R = 0.32$ and $R_w = 0.41$, where $R = \sum ||F_o| - |F_c|| / \sum |F_o|$ and $R_w = (\sum w(|F_o| - |F_c|)^2 / \sum F_o^2)^{1/2}$.

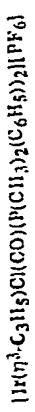
Subsequent difference Fourier syntheses revealed the positions of all nonhydrogen atoms. The nongroup atoms were refined anisotropically; the phenyl rings were treated as rigid groups [30] and restricted to their known geometry ($6/m m m$ symmetry, $d(\text{C}-\text{C}) = 1.395 \text{ \AA}$). The fluorine atoms of the hexafluorophosphate anion were also treated as a rigid group ($m3m$ symmetry, $d(\text{P}-\text{F}) = 1.590 \text{ \AA}$)**. Each group atom was assigned an individual isotropic thermal parameter. Subsequent refinement led to the values $R = 0.064$ and $R_w = 0.092$. A difference Fourier map revealed the positions of all 27 unique hydrogen atoms. This map also suggested an alternative orientation of the hexafluorophosphate ion; this orientation with occupancy $1 - \alpha$ was included with the original orientation (occupancy α) in subsequent calculations. The hydrogen atoms were included in later structure factor calculations in calculated positions ($d(\text{C}-\text{H}) = 0.95 \text{ \AA}$) which were not refined. The allyl hydrogen atoms were found in the plane of the three carbon atoms, and accordingly their positions were idealized in this plane.

After further refinement, a difference Fourier map revealed a valley ($-2 e \text{ \AA}^{-3}$) near the iridium atom and several peaks ($\text{ht.} \approx 1.2 e \text{ \AA}^{-3}$) in the region of

* In addition to various local programs for the CDC 6400, computer programs used in this work include local versions of Zalkin's FORDAP Fourier program, the AGNOST absorption program, and Busing and Levy's ORFFE function and error program. Our least-squares program NUCLS, in its non-group form, closely resembles the Busing-Levy ORFLS program. The diffractometer was run under the disc-oriented Vanderbilt system [28].

** The P-F distance of 1.590 \AA represents an average of the distances in several structures containing the ordered PF_6^- anion.

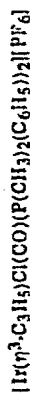
TABLE I. POSITIONAL AND THERMAL PARAMETERS FOR THE NiC₂ GROUP ATOMS OF



ATOM	X	Y	Z	B ¹	K11	B22	R11	R12	B13	R21
IR	-0.195956(43)	0.371548(41)	0.286510(30)	63.95(49)	53.65(42)	34.45(25)	-5.40(35)	12.35(22)	-4.27(24)	
P1	-0.26078(34)	0.37465(30)	0.16204(22)	94.2(21)	69.9(24)	39.5(15)	5.7(25)	12.2(17)	4.1(14)	
P2	-0.26415(28)	0.42031(24)	0.32168(18)	68.7(24)	59.7(22)	28.1(12)	-4.1(20)	5.6(13)	-1.3(12)	
P3	0.19452(36)	0.29471(37)	0.05434(24)	92.6(34)	102.4(35)	39.2(17)	7.2(29)	15.4(14)	-0.4(10)	
CL	-0.01022(29)	0.27203(32)	0.27014(21)	66.5(26)	107.3(31)	47.7(15)	14.7(24)	15.1(15)	-0.0(17)	
N	-0.4286(11)	0.48077(8A)	0.70316(73)	142. (13)	90.5(93)	79.8(78)	43.9(94)	57.4(80)	14.4(44)	
C1	-0.0787(15)	0.5257(13)	0.2893(11)	130. (17)	81. (12)	61.5(84)	-45. (12)	26.2(95)	-14.7(84)	
C2	-0.1024(18)	0.5086(15)	0.1551(12)	192. (25)	84. (16)	92. (11)	-70. (17)	18. (13)	-47. (11)	
C3	-0.0792(18)	0.4112(16)	0.3940(10)	170. (23)	120. (16)	52.2(87)	-60. (18)	19. (11)	-28.2(40)	
C4	-0.3402(15)	0.4399(11)	0.29812(90)	138. (18)	47.5(94)	57.4(77)	14. (11)	42.1(92)	7.9(44)	
C5	-0.4047(21)	0.4448(16)	0.1278(10)	234. (32)	113. (17)	57.0(84)	93. (20)	-19. (13)	-0.7(45)	
C6	-0.1486(19)	0.4437(17)	0.1221(10)	189. (25)	139. (21)	55.7(87)	-20. (20)	38. (11)	40. (11)	
C7	-0.1697(13)	0.1542(12)	0.40293(83)	97. (14)	97. (12)	34.4(60)	14. (11)	-4.5(70)	13.0(64)	
C8	-0.2622(13)	0.0842(11)	0.26534(83)	118. (14)	71.3(49)	40.1(64)	1.3(98)	31.6(75)	-7.0(60)	
F1	0.2028(13)	0.3555(99)	0.12504(71)	450. (14)	325. (14)	64.7(59)	60. (12)	27.4(81)	-32.3(60)	
F2	0.1076(13)	0.36977(97)	0.04777(70)	191. (18)	140. (14)	153.9(59)	-67. (12)	45.1(83)	19.0(60)	
F3	0.4990(13)	0.3882(10)	0.02678(70)	204. (17)	134. (13)	117.8(53)	54. (12)	-4.0(87)	38.0(70)	
F4	0.2878(12)	0.2063(11)	0.08889(66)	174. (17)	140. (13)	134.0(54)	70. (13)	-2.6(78)	49.0(73)	
F5	0.2005(12)	0.2351(11)	-0.00912(68)	189. (14)	114. (13)	104.0(54)	-25. (13)	94.2(77)	-91.0(73)	
F6	0.0825(12)	0.2195(10)	0.05034(66)	156. (17)	154. (13)	125.9(54)	-48. (13)	51.2(78)	55.2(72)	

^A ESTIMATED STANDARD DEVIATIONS IN THE LEAST SIGNIFICANT FIGURE(S) ARE GIVEN IN PARENTHESES IN THIS AND ALL SUBSEQUENT TABLES. THE FORM OF THE ANISOTROPIC THERMAL ELLIPSOID IS: $\text{EAP} = (\text{R}1)^2 + 2\text{H}1\text{R}1\text{R}2 + \text{R}2^2 + 2\text{H}2\text{R}2\text{R}3 + \text{R}3^2$. THE QUANTITIES GIVEN IN THE TABLE ARE THE THERMAL COEFFICIENTS $\times 10^4$.

TABLE 2. DERIVED PARAMETERS FOR THE RIGID GROUP ATOMS OF



ATOM	X	Y	Z	σ^2	ATOM	M	Y	Z	σ^2	R,A
C1R1	-0.28358(8)	0.24462(56)	0.11563(48)	4.00(25)	C1P2	-0.42132(59)	0.21587(70)	0.73549(44)	3.79(24)	
C2R1	-0.40063(68)	0.19513(74)	0.10075(82)	4.52(28)	C2H2	-0.44293(74)	0.22268(80)	0.40281(36)	5.38(11)	
C3R1	-0.41613(74)	0.09166(77)	0.06986(57)	6.46(39)	C3H2	-0.56312(89)	0.25028(87)	0.41108(37)	6.38(17)	
C4R1	-0.3146(10)	0.03767(62)	0.05385(56)	6.35(39)	C4H2	-0.66188(64)	0.245707(84)	0.35203(51)	6.01(13)	
C5R1	-0.19754(83)	0.08715(74)	0.06873(56)	6.26(37)	C5H2	-0.64037(64)	0.24326(80)	0.28470(41)	5.36(11)	
C6R1	-0.18204(63)	0.19063(74)	0.09962(85)	5.08(30)	C6H2	-0.52809(79)	0.22246(73)	0.27643(33)	4.28(15)	

RIGID GROUP PARAMETERS

GROUP	A	X	Y	Z	C	U	DELTA	EPSILON	ETA
R1	-0.2909(63)	0.14114(52)	0.08474(32)	0.08474(32)	-1.5042(56)	2.9032(64)	-0.428(44)		
R2	-0.54100(57)	0.23647(45)	0.34376(32)	0.34376(32)	2.9825(58)	-3.0465(80)	0.3399(49)		

A, X, Y, and Z ARE THE FRACTIONAL COORDINATES OF THE ORIGIN OF THE RIGID GROUP. THE RIGID GROUP ORIENTATION ANGLES DELTA, EPSILON, AND ETA (RADIANS) HAVE BEEN DEFINED PREVIOUSLY; S.J. LA PLACA AND J.A. IBERS, ACTA CRYSTALLOGR. 18, 511(1965).

TABLE 4
ROOT-MEAN-SQUARE AMPLITUDES OF VIBRATION (Å)

Atom	Min.	Intermed.	Max.
Ir	0.185(1)	0.204(1)	0.253(1)
P(1)	0.221(4)	0.239(4)	0.274(5)
P(2)	0.195(4)	0.216(4)	0.233(5)
P(3)	0.231(4)	0.267(6)	0.279(5)
C	0.188(4)	0.288(4)	0.297(5)
C(1)	0.19(2)	0.30(2)	0.35(2)
C(2)	0.15(3)	0.37(3)	0.42(3)
C(3)	0.21(2)	0.32(3)	0.38(2)
C(4)	0.18(2)	0.25(2)	0.34(2)
C(5)	0.20(2)	0.31(2)	0.46(2)
C(6)	0.21(3)	0.34(2)	0.39(2)
C(7)	0.20(2)	0.28(2)	0.30(2)
C(8)	0.22(2)	0.24(2)	0.29(2)
F(1)	0.33(2)	0.46(1)	0.56(1)
F(2)	0.27(2)	0.41(1)	0.54(1)
F(3)	0.25(2)	0.39(1)	0.50(1)
F(4)	0.24(2)	0.40(1)	0.53(1)
F(5)	0.29(2)	0.46(1)	0.57(1)
F(6)	0.21(2)	0.38(1)	0.51(1)

the anion. Since the positions of these peaks suggested a third possible orientation of the hexafluorophosphate ion, we abandoned the two-group model in favor of an unconstrained model for the anion starting from the first orientation. None of our models for the anion changed any of the cation parameters by a statistically significant amount.

The final refinement of 205 variables using 3018 observations resulted in the values: $R = 0.066$ and $R_w = 0.080$. Agreement of $|F_o|$ and $|F_c|$ is poorest for relatively weak, low-angle reflections. This is consistent with our unsuccessful attempts to model the disordered anion. There were several large peaks in the region of the hexafluorophosphate anion in the final difference Fourier map, with the largest being $1.7 \text{ e } \text{Å}^{-3}$. The depth of the valley near the iridium atom was $-2.1 \text{ e } \text{Å}^{-3}$. The error of an observation of unit weight is 3.08 electrons.

The positional, thermal, and group parameters derived from the last cycle of least-squares refinement are given in Table 1, along with the standard deviations estimated from the inverse matrix. The positional parameters of the ring carbon atoms which may be derived from the data in Table 1 are presented in Table 2 together with the thermal parameters as obtained from the last cycle of refinement. The final values of $10 |F_o|$ and $10 |F_c|$ in electrons are given in Table 3*. Table 4 presents the root-mean-square amplitudes of vibration.

* Table 3, the table of structure amplitudes and Table 4, the root-mean-square amplitudes have been deposited as NAPS Document No. 02900 (22 pages). Order from ASIS/NAPS, c/o Microfiche Publications, P.O. Box 3513, Grand Central Station, New York 10017. A copy may be secured by citing the document number, remitting \$5.50 for photocopies or \$3.00 for microfiche. Advance payment is required. Make checks payable to Microfiche Publications. Outside of the United States and Canada postage is \$3.00 for a photocopy or \$1.50 for a fiche.

Description of the structure

The crystal structure consists of discrete, monomeric ions, occupying general positions in space group $P2_1/c$. The inner coordination geometry of the cation is shown in Fig. 2, a stereo view of the cation is presented in Fig. 3, and a stereo view of the unit cell is presented in Fig. 4. The complex may be considered an octahedral Ir(III) complex, with the allyl anion occupying two coordination sites. A selection of distances and angles is given in Table 5.

All the bond distances and angles are within expected ranges. There are no particularly close intermolecular contacts. In the anion, P—F distances range from 1.44(1) to 1.58(1) Å, F—P—F *cis*-angles range from 81.2(7) to 103.4(7)°, and F—P—F *trans*-angles range from 172.5(8) to 174.3(8)°.

Close examination of the final difference map showed no signs of disorder of the chlorine atom and the carbonyl group. The allyl group similarly shows no signs of disorder, the central atom being closer to the carbonyl group than to the chlorine atom, as can be seen in Fig. 3. Variable-temperature proton magnetic resonance spectra of the 2-methylallyl analog indicate that the cation is a dynamic system in solution at room temperature [31]. Because of this, the general shape of the allyl group, and the possibility of an alternative orientation in our mechanism, the order of the allyl group was at first surprising. However, the

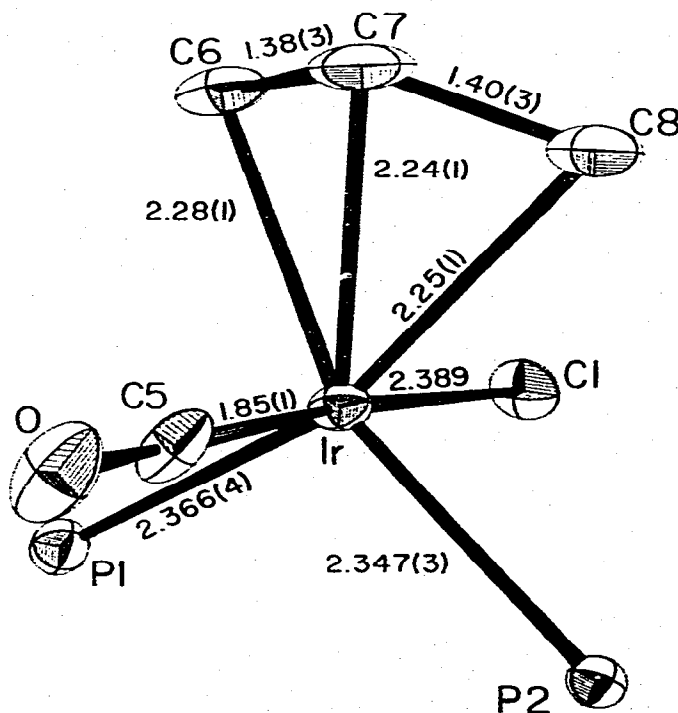


Fig. 2. A perspective view of the coordination geometry about the iridium atom. The shapes of the atoms in this drawing represent 12% probability contours of thermal motion.

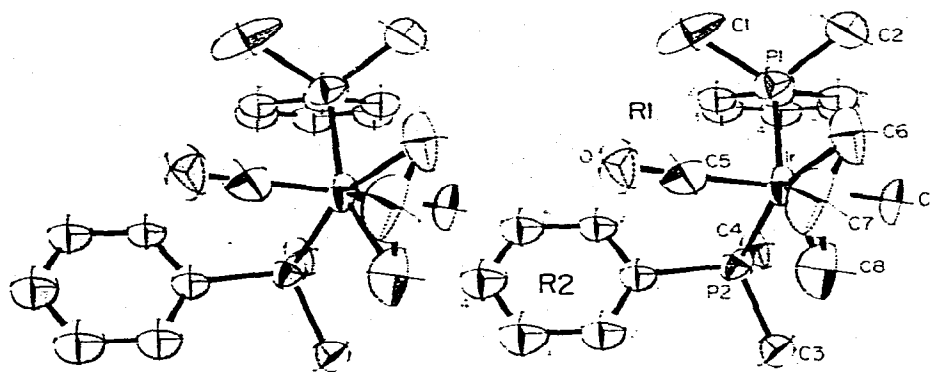


Fig. 3. A stereoview of the cation. The view is approximately along [010]. Hydrogen atoms are omitted. The shapes of the atoms represent 50% probability contours of thermal motion.

general shape of the cation is determined primarily by the phosphine ligands, and the closest intermolecular contacts (see Table 5) of the allyl group involve phosphine ligands. If an alternative orientation of the allyl group is imagined (one with the central carbon atom closer to the chlorine atom and the angle between the allyl plane and the P—Ir—P plane about 120°) several intermolecular contacts much less than the sums of van der Waals' radii result. We therefore attribute the order of the allyl group to crystal packing forces.

A useful comparison can be made between the results presented here and the reported structure of an Ir(I)-(η^3 -allyl) complex, $\text{Ir}(\eta^3\text{-C}_3\text{H}_5)[\text{P}(i\text{-Pr})_3]_2$ [19]. The Ir—P bonds are longer in the Ir(III) complex: 2.347(3) and 2.366(4) Å, vs. 2.270(2) Å in the Ir(I) complex (which has crystallographically-imposed twofold symmetry). The Ir(III)—P bonds are within the normal range. The possibly significant difference in the two chemically equivalent bond distances may arise from differences in the intermolecular contacts involving the phosphine ligands. The Ir(III)—C(allyl) bonds are also longer: Ir(III)—C(terminal) = 2.28(1) and 2.25(1); Ir(I)—C(terminal) = 2.21(2); Ir(III)—C(central) = 2.24(1); Ir(I)—C(central) = 2.10(2) Å. The allyl C—C bonds are similar: 1.38(3) and 1.40(3) Å in the

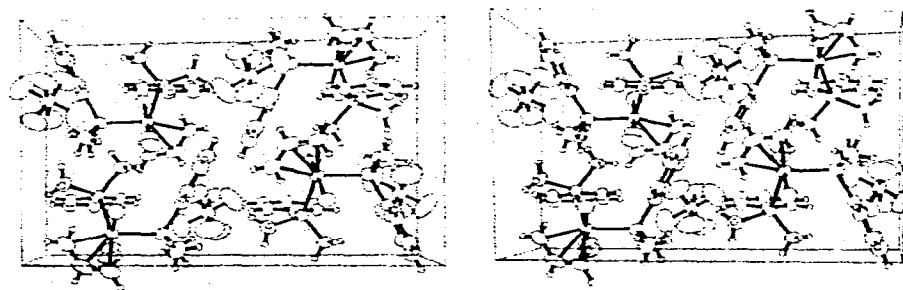


Fig. 4. Stereodrawing of a unit cell of $[\text{Ir}(\eta^3\text{-C}_3\text{H}_5)\text{Cl}(\text{CO})(\text{P}(\text{CH}_3)_2(\text{C}_6\text{H}_5))_2][\text{PF}_6]$. The view is down [100], with the y -axis vertical, and the z -axis horizontal and to the left. Hydrogen atoms are represented by spheres corresponding to a B of 1.0 \AA^2 . The shapes of the atoms represent 40% probability contours of thermal motion.

TABLE 5
SELECTED DISTANCES AND ANGLES

Cation Intramolecular Dist (Å)			
Ir—P(1)	2.366(4)	C(6)—C(7)	1.38(3)
Ir—P(2)	2.347(3)	C(7)—C(8)	1.40(3)
Ir—Cl	2.389(3)	P(1)—C(1)	1.85(2)
Ir—C(5)	1.85(1)	P(1)—C(2)	1.81(2)
Ir—C(6)	2.28(1)	P(1)—C1R1	1.82(1)
Ir—C(7)	2.24(1)	P(2)—C(3)	1.79(1)
Ir—C(8)	2.25(1)	P(2)—C(4)	1.82(1)
		P(2)—C1R2	1.82(1)
Nonbonded Contacts (Å)			
Ir—H2C8	2.18	Ir—H2C6	3.02
Ir—H1C6	2.20	C1—H2C8	2.32
Ir—HC7	2.93	C1—H1C6	2.37
Ir—H1C8	2.96		
Intermolecular Contacts (Å)			
HC3R1—HC4R1	2.40	HC7—F(4)	2.56
H2C1—F(2)	2.52	H1C8—HC5R1	2.49
H3C4—F(1)	2.59	C(7)—HC5R1	2.76
H2C6—Cl	2.65	C(8)—HC5R1	2.84
HC7—F(6)	2.36		
Cation Angles (°)			
P(1)—Ir—P(2)	105.7(1)	Cl—Ir—C(6)	86.9(4)
P(1)—Ir—C(5)	92.9(5)	Cl—Ir—C(7)	100.5(6)
P(2)—Ir—C(5)	91.1(4)	Cl—Ir—C(8)	85.4(6)
P(1)—Ir—Cl	86.4(1)	P(1)—Ir—C(6)	92.8(5)
P(2)—Ir—Cl	85.4(1)	P(2)—Ir—C(8)	94.1(5)
C(5)—Ir—Cl	176.0(4)	C(1)—P(1)—C(2)	104.7(10)
C(6)—Ir—C(7)	35.6(7)	C(1)—P(1)—C1R1	103.6(7)
C(7)—Ir—C(8)	36.4(8)	C(2)—P(1)—C1R1	104.8(7)
C(6)—Ir—C(8)	66.2(6)	C(3)—P(2)—C(4)	100.4(7)
C(5)—Ir—C(6)	97.0(6)	C(3)—P(2)—C1R2	106.3(6)
C(5)—Ir—C(7)	96.6(8)	C(4)—P(2)—C1R2	107.4(6)
C(5)—Ir—C(8)	83.1(7)	C(6)—C(7)—C(8)	125(2)

Ir(III) complex, and 1.38(3) and 1.32(3) Å in the Ir(I) complex. Angles in the coordination spheres of the two complexes are also similar: P—Ir(III)—P = 105.7(1) and P—Ir(I)—P = 110.2(2)°; C(terminal)—Ir(III)—C(terminal) = 66.2(6) and C(terminal)—Ir(I)—C(terminal) = 67.2(2)°; C—C—C(Ir(III)) = 125(2) and C—C—C(Ir(I)) = 129.7(5)°. While no clear conclusions can be drawn from the angles, the trends in bond distances can be interpreted to mean that π -bonding is more important in the Ir(I) complex than in the Ir(III) complex, and that the allyl anion is a better electron acceptor in the Ir(I) complex. The complete planarity of the $C_3H_5^-$ ion in the present structure suggests that the Ir—allyl bonding does not involve significant rehybridization of the carbon atoms.

Structures of $M(\eta^3-C_3H_5)$ complexes

Having verified that the title complex is indeed an η^3 -allyl complex, in support of the proposed mechanism for the addition of allyl halides to $IrX(CO)(PR_3)_2$

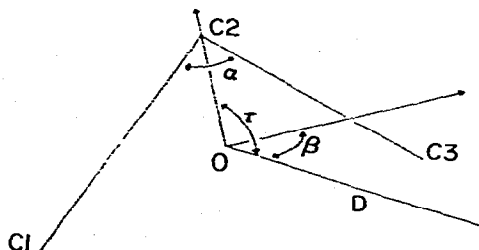


Fig. 5. An illustration of the parameters used to describe the geometry of the metal-allyl linkage. The point O is the center of mass of the allyl group. See text for the definitions of other quantities.

systems, we now examine the nature of the $M-(\eta^3\text{-allyl})$ bond from structural trends. The $M-(\eta^3\text{-allyl})$ linkage is fairly common, and there have been many structures reported containing terminal, unsubstituted allyl groups ($\eta^3\text{-C}_3\text{H}_5$). We limit our attention to these to eliminate as completely as possible such complications as crystal packing forces and ring distortion energies.

To facilitate comparisons, we describe the geometry of the $M-(\eta^3\text{-C}_3\text{H}_5)$ linkage by three parameters which are independent of the geometry and number of other ligands present. The definitions of these parameters are given in Fig. 5. The distance from the metal atom to the center of mass of the allyl group D provides a measure of the average distance of the allyl group from the metal atom. This quantity can be made more useful by modifying it to account for the differences in size among metal atoms. This leads us to define a new quantity D' :

$$\begin{aligned} D' &= D \text{ for 2nd and 3rd-row metals} \\ &= D + 0.10 \text{ \AA for 1st row metals} \end{aligned}$$

The tilt angle τ , the angle between the vector $\overrightarrow{O-M}$ and $\overrightarrow{O-C(2)}$ and the bow angle β , the angle between the vector $\overrightarrow{O-M}$ and the vector parallel to $\overrightarrow{C(1)-C(3)}$ passing through O, describe the orientation of the allyl group.

Pertinent structural parameters of $M-(\eta^3\text{-C}_3\text{H}_5)$ complexes, along with values of D' , τ , and β where it is possible to calculate them, are presented in Table 6. The relatively large variations in most parameters suggest that some useful information may be extracted from them. The near constancy of the bow angle β implies that the deviation from symmetrical π -bonding of the allyl group in these complexes is slight. Several interesting correlations can be discovered among the parameters in Table 6, one being that between D' and \bar{C} , the average C-C distance in the allyl group. This is illustrated in Fig. 6. Although the errors on the parameters involved are large, we believe the correlation to be real. We observe that there are three groups of allyl complexes based on D' , and that these correspond to the groups based on the numbers of metal d electrons*. The negative correlations between \bar{C} and D' for the d^8 and d^4 systems is the expected one, and can

(continued on p. 258)

* The only exception to this grouping is $\text{Mo}(\text{C}_3\text{H}_5)[\text{H}_2\text{B}\{\text{Me}_2\text{pz}\}](\text{CO})_2$ (pz = 1-pyrazolyl), in which there is a short nonbonded Mo-H contact of 2.30 Å, and several very short contacts between the allyl group and the carbonyl groups and pyrazolyl rings [15]. Exceptional behavior can therefore be expected of this compound.

TABLE 6
STRUCTURAL PARAMETERS OF ALLYL COMPLEXES

Compound	M-C central (Å)	M-C end (Å)	C-C-C (°)	C-C (Å)	D' (Å)	τ (°)	β (°)	d ^h ^a	No. o ^{-a}
<i>c</i> /[Mo(C ₃ H ₅)(CO) ₂ (C ₃ H ₅ N)(C ₁₀ H ₈ N ₂)](BF ₄) ⁺	2.279(10)	2.308(8) 2.200(9)	114.8(8)	1.369(13) 1.471(13)	2.05	109.1	90.6	4	18
Mo(C ₃ H ₅)(NCS)(CO) ₂ (C ₁₀ H ₈ N ₂) ^h	2.197(9)	2.291(11) 2.351(12)	115.7(11)	1.440(17) ^c	2.02	103.7	90.9	4	18
Mo(C ₃ H ₅)(pz) ₂ BEt ₂ (CO) ₂ (Hpz) ^l	2.206(3)	2.341(4) 2.347(4)	117.2(4)	1.387(6) 1.412(6)	2.06	102.2	90.3	4	18
Mo ₂ (C ₃ H ₅) ₄ ^{f,i}	2.31(2)	2.29(2) 2.30(2)	120(2)	1.35(3) 1.40(3)	2.06	117.5	90.8	4	16
Cr ₂ (C ₃ H ₅) ₄ ^{f,h}	2.35(2)	2.35(2) 2.28(2)	122(2)	1.38(3) 1.34(3)	2.09	121.1	93.0		
	2.31(5)	2.26(5) 2.24(5)	121	1.46(8) 1.45(8)	2.10	132.2	92.6	4	16
	2.30(5)	2.27(5) 2.19(5)	126	1.31(8) 1.45(8)	2.10	126.2	90.8		
Mo(C ₃ H ₅)(H ₂ B{Me ₂ pz}) ₂ (CO) ₂ ^l	2.214(8)	2.331(8) 2.358(9)	118.4(4)	1.421(12) 1.352(11)	1.96	97.1	92.6	4	16 (187)
[Ir(C ₃ H ₅)(C(CO)(PMe ₂ Ph) ₂)(PF ₆) ^m	2.24(1)	2.28(1) 2.25(1)	125(2)	1.38(3) 1.40(3)	1.99	120.4	90.5	6	18
Ru(C ₃ H ₅) ₂ (PPh) ₂ · C ₇ H ₆ ⁿ	2.13(1)	2.25(2) 2.23(1)	118.2(13)	1.40(3) 1.42(3)	1.94	107.0	90.5	6	18
	2.12(2)	2.24(1) 2.24(2)	120.4(13)	1.39(2) 1.38(2)	1.94	109.2	91.7		
Fe(C ₃ H ₅)(CO) ₃ ^{d,o}	2.09	2.26 2.34	131	1.39 ^c				6	18
[Rh(C ₃ H ₅) ₂ Cl] ₂ ^{d1,f,p}	2.15(2)	2.25(2) 2.12(2)		1.40(3) 1.48(3)				6	16
	2.17(2)	2.12(2) 2.26(2)		1.41(3) 1.45(3)					

$\text{Ir}(\text{C}_3\text{H}_5)_2(\text{P}(-\text{Pr})_2)_2$ ^{b, q}	2.10(2)	2.21(2)	129.7(5)	1.32(3) 1.38(3)	1.91	114.8	91.2	8	16
$[\text{Pd}(\text{C}_3\text{H}_5)\text{Cl}]_2$ ^{e, r} (room temp.)	2.02(4)	2.14(2) 2.17(3)	128.6(33)	1.35(4) 1.37(4)	1.84	112.0	91.4	8	16
$[\text{Pd}(\text{C}_3\text{H}_5)\text{Cl}]_2$ ^{e, r} (-140°C)	2.108(6)	2.123(7) 2.121(8)	119.8(6)	1.357(15) 1.39(2)	1.85	118.1	90.7	8	16
$[\text{Pd}(\text{C}_3\text{H}_5)\text{Cl}]_2 \cdot \text{C}_6\text{H}_{10}\text{NOH}$ ^{f, i}	2.09(2)	2.18(2) 2.12(2)	126.8(18)	1.32(4) 1.34(4)	1.86	127.3	92.2	8	16
$[\text{Ni}(\text{C}_3\text{H}_5)(\text{CH}_4\text{N}_2\text{S}_2)\text{Cl}]$ ^u	1.97(3)	2.04(2) 2.07(2)	123.9(10)	1.40(3) 1.33(3)	1.84	115.5	92.1	8	16
$\text{Ni}_2(\text{C}_3\text{H}_5)_2(\text{C}_8\text{H}_6)$ ^{e, v}	1.92(4)	2.03(4) 2.01(4)	118.5(15)	1.41(4) 1.41(4)	1.79	112.0	90.6	8	18
$\text{Pd}(\text{C}_3\text{H}_5)_2$ ^{ep, d, w}	2.02(3)	2.08(3) 2.08(3)		1.35(4) 1.35(4)				8	18
$[\text{Pd}(\text{C}_3\text{H}_5)\text{OAc}]_2$ ^{d, i, x}	2.05(4)	2.08(4)		1.34(5) 1.37(5) 1.42(5) 1.33(5)				8	16

^a Electrons are counted assuming C_3H_5^- . ^b Crystallographically imposed twofold symmetry. ^c Imposed center of symmetry. ^d Atomic coordinates not available.

^e Average C—C distance. ^f Two independent terminal allyl groups. ^g Ref. 10; $\text{C}_{10}\text{H}_8\text{N}_2 = 2,2'$ -bipyridine. ^h Ref. 11. ⁱ Ref. 12; *pz* = pyrazoly. ^j Ref. 13. ^k Ref. 14. ^l Ref. 15. ^m This work. ⁿ Ref. 16. ^o Ref. 17. ^p Ref. 18. ^q Ref. 19. ^r Ref. 20. ^s Ref. 21. ^t Ref. 22; $\text{C}_6\text{H}_9\text{NOH} = \text{cyclohexanone oxime}$. ^u Ref. 23; $\text{CH}_4\text{N}_2\text{S} = \text{thiourea}$. ^v Ref. 24; $\text{C}_8\text{H}_6 = \text{dihydropentalene}$. ^w Ref. 25. ^x Ref. 26.

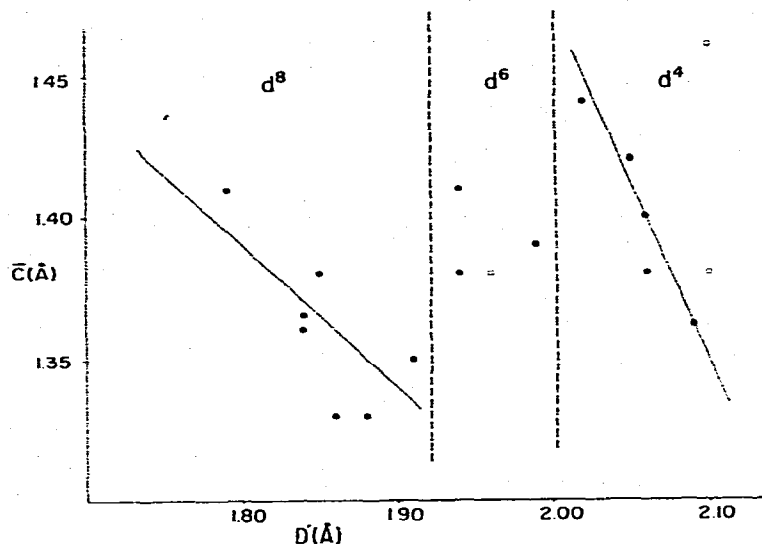


Fig. 6. A plot of \bar{C} , the average C—C distance in the allyl group, versus D' . Shown are unit-weighted least-squares lines: that for the d^8 complexes is $\bar{C} = -0.58 D' + 2.44$, and that for the d^4 complexes is $\bar{C} = -1.19 D' + 3.85$ Å. The open circles represent the allyl groups in $\text{Cr}_2(\text{C}_3\text{H}_5)_4$, which were not included in the calculation because of the large uncertainties. The open square represents the complex $\text{Mo}(\text{C}_3\text{H}_5)(\text{CO})_2[\text{H}_2\text{B}(\text{Me}_2\text{pz})_2]$, which was not included in the calculations.

be rationalized in two ways. A shorter (and therefore presumably stronger) $\text{M}-\text{C}_3\text{H}_5^-$ bond can be the result of either increased electron transfer from the bonding and non-bonding π -orbitals of the allyl anion to the metal atom, or the increased transfer of electrons from a filled metal d orbital into the antibonding allyl π -orbital. The fact that the general order of $\text{M}-\text{C}_3\text{H}_5^-$ bond lengths is $d^8 < d^6 < d^4$ suggests that transfer of electrons from the metal atom plays a substantial role in bonding in these complexes, as the expected strength of back-bonding is $d^8 > d^6 > d^4$. The differences in the bond lengths for these d^8 , d^6 and d^4 complexes may thus reflect the varying relative importance of the two bonding mechanisms. Note that the observed ordering of $\text{M}-\text{C}_3\text{H}_5^-$ bond lengths ($d^8 < d^6 < d^4$) can also be predicted by arguments based on the effective charge felt by the d electrons. We believe that the observed differences in D' (~ 0.1 Å) are too large to be explained completely by these arguments. There are insufficient structural data available to conclude that the trend observed here is common to other similar classes of organometallic complexes (e.g., C_5H_5^- and C_2H_4 complexes).

Perhaps the best correlation is that between α , the C—C—C angle of the allyl group, and D' . This is illustrated in Fig. 7. We can derive several explanations for the observed trends, but believe that, because the slopes of the least-squares lines are nearly identical, the most likely one is the adjustment of the allyl geometry to variations in D' to maximize overlap of the orbitals responsible for M -allyl bonding.

There have been several attempts to provide a theoretical bonding scheme for

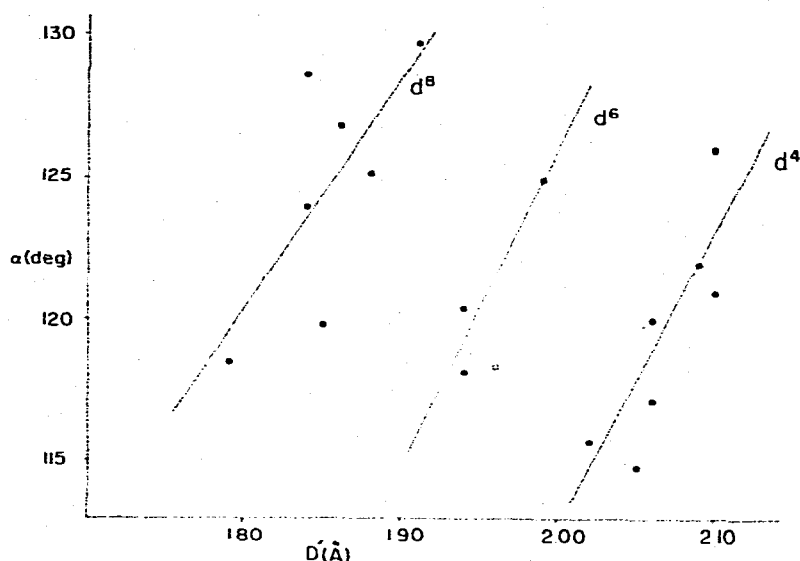


Fig. 7. A plot of α versus D' . The lines are unit-weighted least-squares lines. The open square represents $\text{Mo}(\text{C}_3\text{H}_5)[\text{H}_2\text{B}\{\text{Me}_2\text{pz}\}_2](\text{CO})_2$, which was eliminated from the calculations. The lines are given by the equations: d^8 : $\alpha = 81 D' - 26$; d^6 : $\alpha = 114 D' - 102$; $\alpha = 112 D' - 112^\circ$.

π -allyl transition metal complexes. Kettle and Mason [32] showed that the tilt angle of about 120° in these complexes is the result of the interaction of two separate overlap mechanisms. Thus any picture involving "pure" allyl π - and metal d -orbitals, as we have presented, is oversimplified. They conclude on the basis of the magnitudes of overlap integrals that charge transfer from the metal atom to the π^* allyl orbital is unimportant in M-allyl bonding. Van Leeuwen and Praat [33] provide a similar rationalization of the observed tilt angles, but conclude that M- π^* electron transfer is of some importance in bonding. A more recent calculation on bis(η^3 -allyl)nickel [34] indicates that the transfer of electrons from the non-bonding allyl π -orbital to metal d orbitals is responsible for most of the metal-allyl bonding (in agreement with the earlier workers). These calculations show that backbonding from the metal to the ligand is of some importance, but that the charge transfer does not take place solely between "pure" allyl and metal orbitals. The importance of this backbonding is comparable with that in ferrocene [34].

The transfer of electrons from the non-bonding allyl π -orbital into the metal d orbitals should cause little change in the observed C-C distances. The negative correlation between \bar{C} and D' and the fact that the ordering of D' is $d^8 < d^6 < d^4$ seem difficult to rationalize solely by allyl \rightarrow M electron transfer. The structural data thus suggest that M \rightarrow π^* electron transfer may be more important than previously believed.

Acknowledgments

We wish to thank Matthey-Bishop, Inc., for the generous loan of precious metals used in our studies. We also wish to thank Professor Ralph G. Pearson for

his encouragement and helpful discussions. J.A.K. wishes to acknowledge the support of an NSF predoctoral fellowship. This work was supported by the National Science Foundation.

References

- 1 K.S.Y. Lau, R.W. Fries and J.K. Stille, *J. Amer. Chem. Soc.*, **96** (1974) 4983.
- 2 P.K. Wong, K.S.Y. Lau and J.K. Stille, *J. Amer. Chem. Soc.*, **96** (1974) 5956.
- 3 R.G. Pearson, *Fortschr. Chem. Forsch.*, **41** (1973) 76.
- 4 J.S. Bradley, D.G. Connor, D. Dolphin, J.A. Labinger and J.A. Osborn, *J. Amer. Chem. Soc.*, **94** (1972) 4043.
- 5 J.A. Labinger, A.V. Kramer and J.A. Osborn, *J. Amer. Chem. Soc.*, **95** (1973) 7908.
- 6 J.A. Osborn, in Y. Ishii and M. Tsutsui (Eds.), *Organotransition-Metal Chemistry*, Plenum Publishing Corp., New York, New York, 1975.
- 7 (a) P.B. Chock and J. Halpern, *J. Amer. Chem. Soc.*, **88** (1966) 354; (b) P.B. Chock and J. Halpern, *Proc. Tenth Intl. Conf. Coord. Chem.*, (1967) 135; (c) R.G. Pearson and W.R. Muir, *J. Amer. Chem. Soc.*, **92** (1970) 5519; (d) J.A. Labinger, R.J. Braus, D. Dolphin and J.A. Osborn, *Chem. Commun.*, (1970) 612; (e) F.R. Jensen and B. Knickel, *J. Amer. Chem. Soc.*, **93** (1971) 6339; (f) R. Ugo, A. Pasini, A. Frisi and S. Cenini, *J. Amer. Chem. Soc.*, **94** (1972) 7364; (g) M. Kubota, G.W. Kiefer, R.M. Ishikawa and K.E. Bencala, *Inorg. Chim. Acta*, **7** (1973) 195; (h) H. Stieger and H. Kelm, *J. Phys. Chem.*, **77** (1973) 290; (i) J. Burgess, M.J. Hacker and R.D.W. Kemmitt, *J. Organometal. Chem.*, **72** (1974) 121.
- 8 A.J. Deeming and B.L. Shaw, *J. Chem. Soc. A*, (1969) 1562.
- 9 A.T. Poulos and R.G. Pearson, unpublished results.
- 10 R.H. Fenn and A.J. Graham, *J. Organometal. Chem.*, **37** (1972) 137.
- 11 A.J. Graham and R.H. Fenn, *J. Organometal. Chem.*, **17** (1969) 405.
- 12 F.A. Cotton, B.A. Frenz and A.G. Stanislowski, *Inorg. Chim. Acta*, **7** (1973) 503.
- 13 F.A. Cotton and J.R. Pipal, *J. Amer. Chem. Soc.*, **93** (1971) 5441.
- 14 T. Aoki, A. Furusaki, Y. Tonire, K. Ono and K. Tanaka, *Bull. Chem. Soc. Japan*, **42** (1969) 545.
- 15 C.A. Kosky, P. Gaius and G. Avitable, *Acta Crystallogr.*, **B27**, (1971) 1859.
- 16 A.E. Smith, *Inorg. Chem.*, **11** (1972) 2306.
- 17 M.Kh. Minasyan, Yu.T. Struchkov, I.I. Kritskaya and R.L. Avoyan, *J. Struct. Chem.*, **7** (1966) 840.
- 18 M. McParthin and R. Mason, *Chem. Commun.*, (1967) 16.
- 19 G. Perego, G. Del Piero and M. Cesari, *Cryst. Struct. Commun.*, **3** (1974) 721.
- 20 W.E. Oberhanski and L.F. Dahl, *J. Organometal. Chem.*, **3** (1965) 43.
- 21 A.E. Smith, *Acta Crystallogr.*, **18** (1965) 331.
- 22 Y. Kitano, T. Kajimoto, M. Kashiwagi and Y. Kinoshita, *J. Organometal. Chem.*, **33** (1971) 123.
- 23 A. Sirign, *Inorg. Chem.*, **9** (1970) 2245.
- 24 Y. Kitano, M. Kashiwagi and Y. Kinoshita, *Bull. Chem. Soc. Japan*, **46** (1973) 723.
- 25 M.Kh. Minasyan, S.P. Fubin and Yu.T. Struchkov, *J. Struct. Chem.*, **7** (1966) 843.
- 26 M.R. Churchill and R. Mason, *Nature*, **204** (1964) 777.
- 27 R.J. Doedens and J.A. Ibers, *Inorg. Chem.*, **6** (1967) 204.
- 28 P.G. Lenhert, *J. Appl. Crystallogr.*, **8** (1975) 568.
- 29 D.T. Cromer and J.T. Waber, *International Tables for X-ray Crystallography*, Vol. IV, Kynoch Press, Birmingham, England, 1974. Table 2.2A: D.T. Cromer, *Ibid.*, Table 2.3.1.
- 30 See, for example, R. Eisenberg and J.A. Ibers, *Inorg. Chem.*, **4** (1965) 773.
- 31 A.T. Poulos, unpublished results.
- 32 S.F.A. Kettle and R. Mason, *J. Organometal. Chem.*, **5** (1966) 573.
- 33 P.W.N.M. van Leeuwen and A.P. Praat, *J. Organometal. Chem.*, **21** (1970) 501.
- 34 M.-M. Rohmer, J. Demuyneck and A. Veillard, *Theoret. Chim. Acta*, **36** (1974) 93.